JURNAL KIMIA VALENSI
p-ISSN: 2460-6065; e-ISSN: 2548-3013
Journal homepage: https://journal.uinjkt.ac.id/index.php/valensi
Research Article

Synthesis and Characterization of Hydroxyapatite-Ag Nanocomposites Using Areca Nut Peel Bioreductors (*Areca catechu* L.) for Antibacterial Applications

Restina Bemis[1]*, Heriyanti[1], Ratih Dyah Puspita Sari[1], Nurul Pratiwi[1] and Levi Febiola Aulia Putri[1]

[1]*Department of Chemistry, Faculty of Science and Technology, Universitas Jambi, Jambi (36361), Indonesia*

Email: restina@unja.ac.id

Article Info
Received: July 12, 2023
Revised: September 14, 2023
Accepted: November 24, 2023
Online: November 30, 2023

Citation:
Bemis, R., Heriyanti, Sari, R. D. P., Pratiwi, N., & Putri, L. F. A. (2023). Synthesis and Characterization of Hydroxyapatite-Ag Nanocomposites Using Areca Nut Peel Bioreductors (Areca catechu L.) for Antibacterial Applications. *Jurnal Kimia Valensi*, 9(2), 216-223. Doi: 10.15408/jkv.v9i2.32638

Abstract
Calcium Hydroxyapatite (HAp, $Ca_{10}(PO_4)_6(OH)_2$) is an important material utilized in bone, tooth enamel, and dentin. In this study, areca nut peel bioreductors (Areca catechu L.) were used to synthesize HAp-Ag nanocomposites using green synthesis method. The effect of polyvinyl alcohol (PVA) amount on the structure and morphologies of the synthesized HAp-Ag nanocomposites were investigated. The XRD showed that the crystal size of synthesized HAp-Ag nanocomposites is 1-100 nm with a degree of crystallinity above 60%. SEM images showed that the particles of HAp-Ag nanocomposites were nano-sized with uneven spherical shape. The antibacterial activity test was carried out against *Staphylococcus aureus* and *Escherichia coli* using the disc diffusion test. The result showed that Ag NPs incorporated in modified HAp inhibited Gram-negative bacteria more efficiently than Gram-Positive bacteria. Based on the antibacterial test results, the hydroxyapatites were effective against all tested microorganisms. Therefore, it can be considered as an antimicrobial biomaterial that can be used in implant and reconstructive surgery applications.

Keywords: hydroxyapatite, silver nanoparticle, antibacterial

1. INTRODUCTION

Calcium, as one of the many essential elements, can be processed into hydroxyapatite. According to Ngatijo et al. (2021), XRF analysis results revealed that calcium dominated PCC from rebon shrimp, comprising 70.8% calcium, 12.3% phosphorus, and 4.32% potassium. Hydroxyapatite (HAp, $Ca_{10}(PO_4)_6(OH)_2$) is an important material used for bone, tooth enamel and dentin. Notably, hydroxyapatite composites incorporating Sr, Zn, Ce, and Ag have been developed due to their excellent biocompatibility (LeGeros, 1991). The hydrothermal synthesis method is employed to produce hydroxyapatite powder, ensuring high purity and quality even at low temperatures (Kusnieruk *et al*., 2016).

In particular, silver (Ag) nanoparticles have attracted a lot of attention in the scientific field. Various methods, including the chemical reduction method using toxic reagents like $NaBH_4$, have been employed. However, the environmental impact has led to the development of green synthesis methods, utilizing bio-organisms as reducing agents. In this context, Polyvinyl Alcohol (PVA) serves as a stabilizing agent due to its non-toxic, water-soluble, and biocompatible properties, preventing unwanted agglomeration and oxidation (Apriandanu *et al*., 2013). Bioreductors from plant extracts can be utilized to reduce Ag^+ ions to Ag^0 involving secondary metabolites (Choi *et al*., 2021).

One of the plants originating from Jambi Province which has potential as a bioreductor is Areca nut. Areca nut (*Areca catechu* L.) peel contains secondary metabolites such as flavonoids, alkaloids, tannins, and triterpenoids (Pribady *et al*., 2019). Areca nut is widely used as an ingredient for stomach and headache medicine, as a cosmetic and as an ingredient in traditional ceremonies. Areca nut also has antioxidant activity, antidepressant activity, and antibacterial activity (Andesmora, 2021). However, the Areca nut peel has not been used properly so it only ends up as waste. Therefore, this study utilizes the areca nut peel as a

bioreductor for Ag, aiming to synthesize HAp-Ag nanocomposites as biomaterials with antibacterial properties.

2. RESEARCH METHODS

Instrumentations and Materials

The instruments used in this research were X-Ray Diffraction (XRD), Scanning Electron Microscope (SEM), and Fourier Transform Infrared Spectrometer (FTIR). The materials used in this study were Areca nut peel, rebon shrimp, HNO_3 (p.a Merck), NH_4OH (p.a Merck), baking soda (technical), citric acid (technical), distilled water, $(NH_4)_2HPO_4$ (p.a Merck), $AgNO_3$ (p.a Merck), 96% ethanol (p.a Merck), methanol (p.a Merck), sulfuric acid (p.a Merck), Meyer's reagent, Dragendorff's reagent, HCl (p.a Merck), Mg powder (p.a Merck), $FeCl_3$ (p.a Merck), Liebermann-Burchard reagent, polyvinyl alcohol (PVA) (p.a), Nutrient Agar (NA), *Staphylococcus aureus* bacteria, and *Escherichia coli*.

Preparation of Rebon Shrimp Sample

The rebon shrimp samples were dried in an oven, blended and sieved to form a fine, white dry powder. The obtained powder was weighed and calcined at 900°C to convert $CaCO_3$ to CaO (Kadouche *et al*., 2012).

Synthesis of PCC (Precipitated Calcium Carbonate)

The obtained CaO was dissolved with 2M HNO_3, stirred for 30 minutes and filtered. The filtrate was heated at 60°C and pH adjusted to 12 with the addition of concentrated NH_4OH and then filtered again. The filtrate was precipitated by adding CO_2 gas slowly until the pH 8 and a white precipitate were obtained, namely PCC. The obtained precipitate was then filtered and washed with distilled water until pH 7 and then dried in an oven (Harahap *et al*., 2015).

Synthesis of Hydroxyapatite (HAp)

The synthesis of HAp was carried out by mixing PCC and $(NH_4)_2HPO_4$ at Ca/P ratio of 1.73 with pH 11 in 100 mL of distilled water and then concentrated NH_4OH solution was added. This synthesize process was carried out in a hydrothermal vessel at 170°C for 8 hours. Furthermore, the purification step was carried out by filtering the HAp mixture from the remaining reactants using filter paper. The obtained precipitate was then dried at 110°C and weighed to a constant weight (Harahap et al., 2015).

Extraction

Areca nut peel samples were washed and cut into small pieces and then dried at room temperature for 2 days. The dried sample was mashed using a blender and then sieved with a 30-mesh sieve and weighed as much as 25 g. After that, samples were prepared using the maceration method using 250 mL ethanol solvent for 72 hours (Hidayah *et al*., 2019). After that, the phytochemical test was carried out on the extract.

Synthesis of Silver Nanoparticles

Synthesis of Ag nanoparticles was carried out by reacting 50 mL of Areca nut peel bioreductor extracted using ethanol solution. A 200 mL of $AgNO_3$ 0.05 M and 60 mL of PVA with a concentration of 1%, 3%, and 5% were added. The solution then stirred for 2 hours at room temperature. The formation of Ag nanoparticles was visually detected by color changing of the solution from yellowish to brownish (Prasetiowati *et al*., 2018).

Synthesis of HAp-Ag Nanocomposites

HAp-Ag nanocomposites were synthesized by mixing 2 g of HAp powder with 4 mL of various Ag nanoparticle solutions containing 1%, 3%, and 5% PVA concentration. The mixing was carried out at room temperature for 2 hours with constant stirring. Following this, the solution was filtered, and the precipitates were dried at 100°C for 4 hours. Subsequently, characterization was performed using XRD, SEM, and FTIR (Holguin and Lopez, 2020).

Antibacterial Activity Test

Qualitative testing of antibacterial activity was carried out using the disc diffusion test. The HAp-Ag nanocomposites were weighed 0.05 g for the antibacterial activity test. Subsequently, it was applied to the surface of Nutrient Agar (NA) media, which had been previously colonized with the test bacteria *Escherichia coli* and *Staphylococcus aureus*. The setup was then incubated for 24 hours at 37 ℃. As a positive control, paper discs were soaked with tetracycline antibiotics and negative controls were soaked with water. The inhibitory effectiveness was determined by the discernible presence of clear zones surrounding the paper discs. Simultaneously, a quantitative assessment of antimicrobial activity was conducted by calculating the percentage reduction in the bacterial culture (Holguin and Lopez, 2020).

3. RESULTS AND DISCUSSION

Synthesis of Hydroxyapatite (HAp)

Preparation of PCC involved utilizing raw materials containing CaO, which were subsequently dissolved in HNO_3. The inclusion of HNO_3 is essential to generate high-quality PCC precipitates, given its effective reaction with metal oxides present in calcium oxide. The reaction occurring in the preparation of PCC with the acid solution is represented by the following equation (1-3).

$$CaO_{(s)} + HNO_{3(aq)} \rightarrow Ca(NO_3)_{2(aq)} + H_2O_{(l)} \quad (1)$$

$$Ca(NO_3)_{2(aq)} + 2NH_4OH_{(aq)} \rightarrow Ca(OH)_{2(aq)} + 2NH_4NO_{3(aq)} \quad (2)$$

$$Ca(OH)_{2(aq)} + CO_{2(g)} \rightarrow CaCO_{3(s)} + H_2O_{(aq)} \quad (3)$$

Synthesis of HAp was carried out by reacting PCC and $(NH_4)_2HPO_4$ at pH 11 using hydrothermal method. The reaction occurring in this synthesis process is represented by the following equation (4).

$$10CaCO_3 + 6(NH_4)_2HPO_4 + 2H_2O \rightarrow Ca_{10}(PO_4)_6(OH)_2 + 6(NH_4)_2CO_3 + 4H_2CO_3 \quad (4)$$

Synthesis of HAp-Ag Nanocomposites

The synthesis of HAp-Ag nanocomposites initiated with an examination of the Areca nut peel through phytochemical screening. This screening aimed to identify and characterize the bioactive compounds inherent in the sample. The outcomes of the screening test, as outlined in Table 1, indicate the presence of various bioactive compounds, including alkaloids, flavonoids, phenolics/tannins, and triterpenoids within the Areca nut peel. These compounds play a crucial role in subsequent stages of the synthesis, contributing to the overall properties and potential applications of the HAp-Ag nanocomposites.

Table 1. Phytochemical screening of areca nut peel (*Areca catechu L.*)

Test Compound	Test Results
Alkaloid	+
Flavonoid	+
Saponin	-
Steroids	-
Phenolics/Tannins	+
Triterpenoids	+

Simultaneously, the synthesis of Ag nanoparticles was conducted using the green synthesis reduction method. The underlying principle of Ag nanoparticle synthesis through green synthesis involves the utilization of biological materials found in plants, which act as bioreductors to reduce Ag^+ species to Ag^0. In this study, Areca nut peels were employed, containing flavonoid compounds that function as bioreductors. The inclusion of PVA as a stabilizer aimed to prevent the aggregation of nanoparticles. PVA, a polymer, serves to hinder undesirable agglomeration and oxidation processes (Prasetiowati et al., 2018). The formation of Ag nanoparticles was visually detected by color changing of the solution from yellowish to brownish. The mechanism governing the formation of Ag nanoparticles by flavonoids is illustrated in Figure 1.

Referring to the Figure 1, flavonoid compounds undergo group changes to transform into R-O• groups and R-OH groups. Subsequently, they form an RO-Ag group by binding to Ag^+ ions. In this reaction, the flavonoid chain is broken as Ag^+ ions bind and are released, resulting in the formation of Ag nanoparticles (Zakir *et al*., 2014). The mechanism illustrating the formation of the HAp-Ag nanocomposites is depicted in Figure 2.

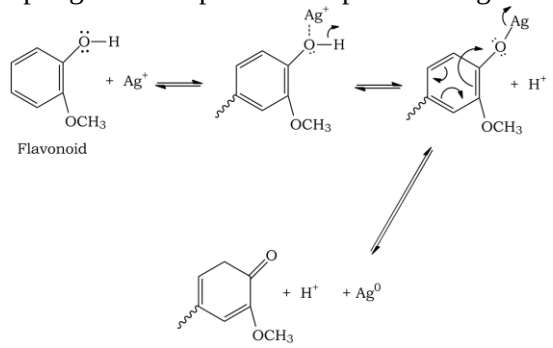

Figure 1. The formation mechanism of Ag nanoparticle

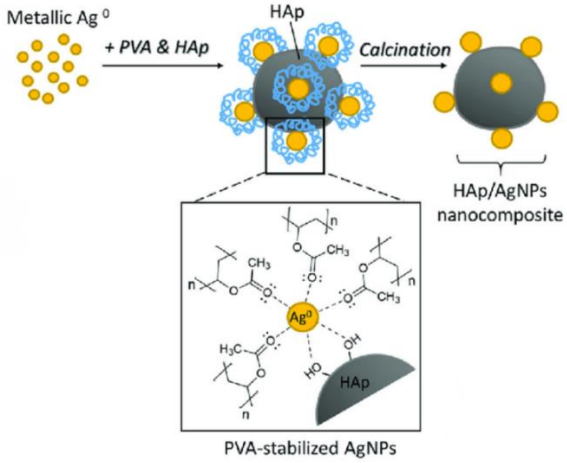

Figure 2. HAp-Ag nanocomposites formation mechanism (Bee *et al*., 2021)

It shows that when Ag metal solution is added to HAp, PVA plays a crucial role in stabilizing Ag, inhibiting excessive agglomeration of Ag particles in the reaction mixture. The strong connection between the surface of the Ag nanoparticles and the oxygen atoms in PVA generates a closed protective layer on the surface of the Ag nanoparticles, inhibiting particle agglomeration by providing a steric repulsive force between the Ag nanoparticles. Meanwhile, HAp in the reaction mixture functions as a nucleation site for the attachment and deposition of Ag nanoparticles. The electron-rich–OH groups on the HAp surface exhibit a high affinity for the Ag atoms, allowing the adsorption and coordination of the Ag atoms through the oxygen atoms on the HAp (Bee *et al*., 2021).

Characterization of HAp-Ag Nanocomposites

Fourier Transform Infrared Spectrometer (FTIR)

In order to determine the functional groups that are present in the synthesized HAp-Ag nanocomposites, characterization was conducted using FTIR. Figure 3 illustrates the absorption spectrum depicting the identified functional groups within the HAp-Ag nanocomposites.

Analyzing the data from the HAp-Ag nanocomposites, as depicted in Figure 3, the FTIR spectrum was conducted within the wavenumber range between 4000-400 cm^{-1}. Multiple functional groups were identified within the HAp-Ag nanocomposites. Starting from the left wavenumber region, O-H stretching groups at wavenumbers 3550-3200 cm^{-1} were observed, originating from the alcohol in the solvent used. Additionally, the OH group is a characteristic feature of compounds found in flavonoids, tannins, terpenoids, and polyphenols. The presence of O-H groups signifies the reduction of Ag^{+} to Ag^{0}, leading to the formation of Ag nanoparticles. Strong O-H vibration is evident in the broad region between 3200-3600 cm^{-1} (Ciobanu *et al*., 2011). Phenolic compounds exhibit absorption areas at wave numbers 1700-1600 cm^{-1}, corresponding to C=O absorption. Within the range of 1700-1400 cm^{-1}, indications of the CO_3^{2-} functional group, present in HAp, are observed. Furthermore, the phosphate functional group, characteristic of HAp, is identified at wave numbers 600-350 cm^{-1} (Hariyanto *et al*., 2019). The absorption band at 570 cm^{-1} is attributed to the asymmetric and symmetric stretching vibration of the P–O bond from the PO_4^{3-} group (Ni *et al*., 2018). These identified functional groups provide valuable insights into the composition and structural properties of the HAp-Ag nanocomposites.

Scanning Electron Microscope (SEM)

SEM analysis was conducted to examine the surface morphology of the HAp-Ag nanocomposites. The obtained SEM results are presented as images illustrating the morphological structure of each sample, with a magnification of 10000x (Figure 4).

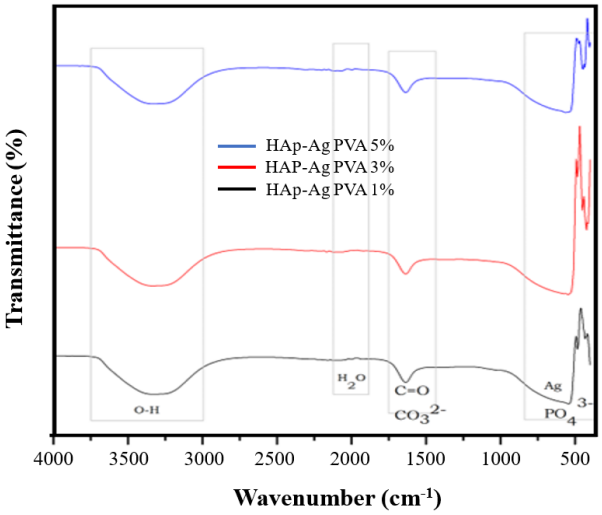

Figure 3. IR spectra of HAp-Ag Nanocomposites

Table 2. Comparative analysis of IR Spectra between synthesized HAp-Ag nanocomposites and HAp-Ag in the literature

Functional Group	Wavenumber (cm^{-1})				
	HAp-Ag with 1% PVA	HAp-Ag with 3% PVA	HAp-Ag with 5% PVA	Ciobanu *et al*, (2011)	Ni *et al*, (2018)
O-H	3327.41	3337.21	3331.22	3432	3572
CO_3^{2-}, C=O	1636.85	1636.60	1636.69	1642	1634
$PO4^{3-}$	541.04	547.70	564.19	563	570

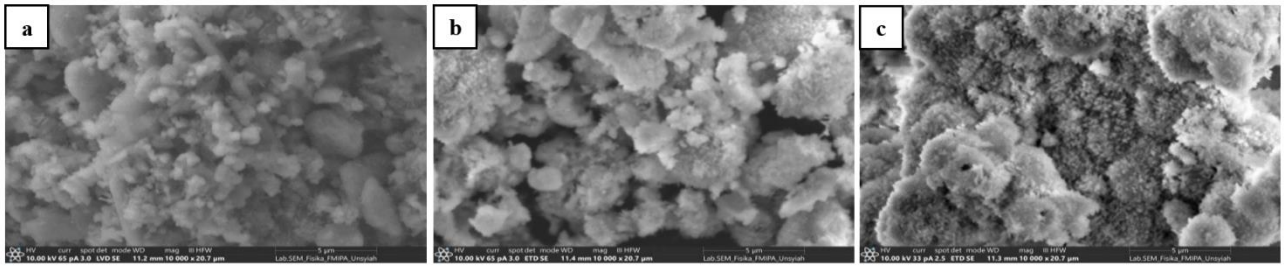

Figure 4. SEM image of HAp-Ag nanocomposites with (a) 1% PVA; (b) 3% PVA; (c) 5% PVA

Utilizing SEM images, as illustrated in Figure 4(a-c), we observed the morphology of HAp-Ag nanocomposites with a magnification of 10000x. The analysis revealed distinct particle sizes and uneven particle distribution. Notably, particles tended to accumulate into chunks, forming agglomerations with diverse spherical morphologies. In this study, SEM image analysis was conducted using the ImageJ and OriginLab programs. Measurements performed with these programs indicated that the particle size of the HAp-Ag nanocomposites with 1% PVA was obtained in the range of 11-32 nm. Meanwhile, the HAp-Ag nanocomposites with 3% PVA and the HAp -Ag nanocomposites with 5% PVA exhibited particle sizes ranging from 11-29 nm and 11-26 nm, respectively. These findings confirm that the resulting HAp nanocomposites possess a nanometer-scale size. In accordance with the research conducted by Holguin and Lopez (2020), the SEM results of the HAp-Ag nanocomposites substantiate the presence of Ag nanoparticles, exhibiting a spherical shape across the entire surface of the HAp.

X-Ray Diffraction (XRD)

The results of characterization using the XRD instrument are used to identify the degree of crystallinity and can also be used to determine crystal size using the Scherrer equation.

Figure 5 shows XRD pattern of HAp-Ag nanocomposites with various concentration of PVA. The XRD pattern of HAp-Ag nanocomposites with 1% PVA shows that peaks at 2θ for HAp are 29.66°; 31.94°; and 32.94° with hkl values (210), (211), and (300) (JCPDS 01-075-9526). While the peaks for Ag are found to exist at 2θ of 35.96° and 46.81° with hkl values (100) and (103) (JCPDS 00-041-1402). By calculating using the Scherrer equation, the average crystal size of the HAp-Ag nanocomposites with 1% PVA is 20.19 nm with the crystallinity degree about 61.32%. The XRD pattern of HAp-Ag nanocomposites with 3% PVA shows that peaks at 2θ for HAp are 25.93°; 31.77°; 32.94°; and 49.55° with hkl values (002), (211), (300), and (213) (JCPDS 01-075-9526). The peaks for Ag are found to exist at 2θ of 34.10° and 46.75° with hkl values (100) and (103) (JCPDS 00-041-1402). It was shown that the average crystal size of the HAp-Ag nanocomposites with 3% PVA is 26.90 nm with crystallinity degree 61.35%. The XRD pattern of HAp-Ag nanocomposites with 1% PVA shows that peaks at 2θ for HAp are 25.89°; 29.52°; 31.75°; and 32.91° with hkl values (002), (210), (211), and (300) (JCPDS 01-075-9526). The peaks for Ag are found to exist at 2θ of 35.92°, 39.77° and 46.72° with hkl values (100), (102) and (103) (JCPDS 00-041-1402). The average crystal size of the HAp-Ag nanocomposites with 5% PVA is 26.90 nm with the crystallinity degree 63.19%. It is known that the crystal structure of the HAp-Ag nanocomposites using Match! program is hexagonal (Mirzaee *et al*., 2016). The obtained results show that the addition of PVA affects the crystal size and crystallinity degree.

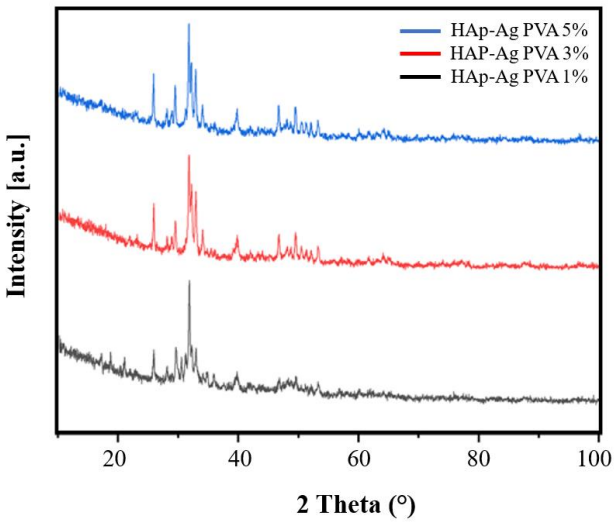

Figure 5. XRD pattern of HAp-Ag nanocomposites

Antibacterial Activity Test

The assessment of antibacterial activity involves analyzing the size and diameter of inhibition zones observed on the agar plate. The dimensions of these inhibition zones are denoted as D (mm), representing the diameter of the inhibition ring (mm). Antibacterial properties are indicated when the diameter of the antibacterial ring is larger

than 2 mm. A ring diameter of less than 5 mm corresponds to weak resistance, while a range of 5–10 mm corresponds to average resistance, and a diameter exceeding 10 mm indicates strong resistance (Pham *et al*., 2020).

The antibacterial test was carried out on the synthesized HAp and HAp-Ag nanocomposites with 5% PVA. The obtained inhibition zone data can be seen in Table 3. Table 3 presents the antibacterial activity of HAp-Ag nanocomposites against *Staphylococcus aureus* and *Escherichia coli* using the disc diffusion test. As depicted in Table 3, the HAp-Ag nanocomposites demonstrated effectiveness against all tested microorganisms. Specifically, the inhibitory zone recorded for Gram-positive Staphylococcus aureus bacteria reached 11.1 mm, while for Gram-negative Escherichia coli, the inhibitory zone reached 12.2 mm. These results indicate a significant antibacterial activity of the HAp-Ag nanocomposites against both bacterial strains, in contrast to HAp, which showed no ability to repress the growth of the bacterial strains (Figure 6).

For comparison, Pham et al. (2020) synthesized HAp-Ag using Centella asiatica (L.) Urban extract and eggshell as precursors. The resulting HAp-Ag was assessed for its antibacterial activity against *Staphylococcus aureus* and *Escherichia coli*, revealing inhibitory zones of 17 mm and 10 mm, respectively. Similarly, Diaz et al. (2009) employed a colloidal chemical route to synthesize HAp-Ag. The test results demonstrated inhibition zones of approximately 17 mm and 18 mm for *Staphylococcus aureus* and *Escherichia coli*, respectively. In another study, Said et al. (2021) synthesized HAp-Ag using ginger oil, and the samples exhibited notable antibacterial properties against *Staphylococcus aureus* and *Escherichia coli*, with inhibitory zones measuring 18 mm and 20 mm, respectively.

The HAp-Ag nanocomposites demonstrate robust antibacterial activity, wherein bacterial cells are drawn to the HAp surface through electrostatic forces. This interaction occurs directly between the bacterial cell membrane and Ag^+ ions. Various studies have corroborated the antimicrobial efficacy of Ag nanoparticles against diverse microorganisms. While the mechanisms underlying this property are multifaceted, it is primarily attributed to the dissolution of Ag nanoparticles and subsequent release of Ag^+ ions. These ions can engage with the negatively charged microbial membrane, impeding their growth through electrostatic attractions. Additionally, Ag^+ ions can react with the –SH groups of microbial enzymes, leading to inhibition. Furthermore, Ag nanoparticles can penetrate microorganisms, inducing DNA damage.

The findings reveal that Ag nanoparticles incorporated into the modified HAp exhibit more pronounced inhibition against Gram-negative bacteria compared to Gram-positive bacteria. This discrepancy can be elucidated by the electrostatic attraction between positively charged Ag^+ ions and negatively charged Gram-negative cell membranes, facilitating the attachment of Ag^+ ions to the membrane. (Said *et al*., 2021).

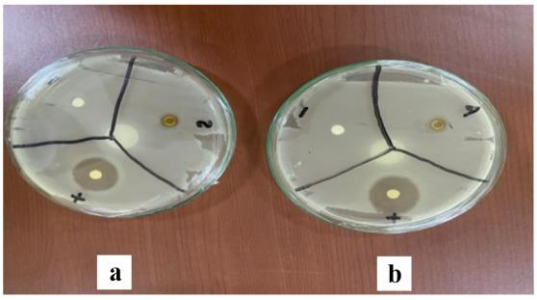

Figure 6. Antibacterial Activity of HAp-Ag nanocomposites against (a) *Staphylococcus aureus* and (b) *Escherichia coli*

Table 3. Antibacterial Activity Test

Type of Bacteria	Clear Zone Diameter (mm)						
	Control		HAp-Ag PVA 5%	HAp	HAp-Ag (Pham *et al*)	HAp-Ag (Diaz *et al*)	HAp-Ag (Said *et al*)
	+	-					
S. aureus	20.1	0	11.1	0	17.0	17	18
E. coli	15.3	0	12.2	0	10.0	18	20

4. CONCLUSIONS

The synthesis of HAp-Ag nanocomposites utilizing Areca nut peel bioreductors (Areca catechu L.) was accomplished through reduction methods and hydrothermal techniques for synthesizing Ag nanoparticles and Hap, respectively. The characterization results of the HAp-Ag nanocomposites using the XRD revealed nanocrystal sizes ranging from 1 to 100 nm, with a degree of crystallinity exceeding 60%. In SEM analysis, particle agglomeration was observed, indicating a spherical morphology with varying sizes in the samples. The FTIR analysis identified that Hap-Ag confirms some functional groups, including O-H, CO_3^{2-}, PO_4^{3-}, and Ag. The antibacterial activity test demonstrated that the HAp-Ag nanocomposite exhibits antibacterial properties against both *Staphylococcus aureus* and *Escherichia coli*. This synthesis process, employing Areca nut peel bioreductors, has proven effective in producing HAp-Ag nanocomposites with well-defined characteristics, showcasing potential applications in antimicrobial settings.

REFERENCES

1. Achmadi, S. 2000. *Jendela IPTEK*. Balai Pustaka. Jakarta.

2. Andesmora, E.V. 2021. "Potensi Budidaya Tanaman Pinang (*Areca catechu L.*) di Lahan Gambut: Studi Kasus di KHG Mendahara Kabupaten Tanjung Jabung Timur, Jambi". *Jurnal Ilmu Pertanian Tirtayasa*. Vol 3(1):219-227.

3. Apriandanu, D.O.B., S. Wahyuni., S. Hadisaputro and Harjono. 2013. "Sintesis Nanopartikel Perak Menggunakan Metode Poliol Dengan Agen Stabilisator Polivinilalkohol (PVA)". *Jurnal MIPA*. Vol 36(2):157-168.

4. Bee, S.L., Y. Bustami., A.U. Hamid., K. Lim and Z.A.A. Hamid. 2021. "Synthesis of silver nanoparticle-decorated hydroxyapatite nanocomposite with combined bioactivity and antibacterial properties". *Journal of Materials Science: Materials in Medicine*. Vol 32(106):1-12.

5. Choi, J.S., H.C. Jung., Y.J. Baek., B.Y. Kim., M.W. Lee., H.D. Kim and S.W. Kim. 2021. "Antibacterial Activity of Green-Synthesized Silver Nanoparticles Using *Areca catechu* Extract against Antibiotic-Resistant Bacteria". *Nanomaterials*. Vol 11:1-16.

6. Ciobanu, C.S., F. Massuyeau., LV. Constantin and D. Predoi. "Stuctural and physical properties of antibacterial Ag-doped nano-hydroxyapatite synthesized at 100°C". *Nanoscale Research Letters*. Vol 6(613):1-8.

7. Diaz, M., F. Barba., M. Miranda., F. Guitian., R. Torrecillas and J. S. Moya. 2009. "Synthesis and Antimicrobial Activity of a Silver-Hidroxyapatite Nanocomposite". *Journal of Nanomaterials*. 1-6.

8. Harahap, A.W., Z. Helwani., Zultiniar and Yelmida. 2015. "Sintesis Hidroksiapatit melalui *Precipitated Calcium Carbonate* (PCC) Cangkang Kerang Darah dengan Metode Hidrotermal pada Variasi pH dan Waktu Reaksi". *Jom FTEKNIK*. Vol 2(2):1-8.

9. Hariyanto, Y.A., A. Taufiq., Sunaryono., N. Mufti., S. Soontaranon and N. Kamonsutthipaijit. 2019. "Study on Structural Characters of Nano-sized Hydroxyapatite Prepared from Limestone". *IOP Conf. Series: Materials Science and Engineering*. Vol 515:1-8.

10. Hidayah, N., A.H. Alimuddin dan Harlia. 2019. "Aktivitas Antioksidan dan Kandungan Fitokimia Dari Ekstrak Kulit Buah Pinang Sirih Muda dan Tua (*Areca catechu L*)". *Jurnal Kimia Khatulistiwa*. Vol 8(2):52-60.

11. Holguin, P.N.S and S.Y.R. Lopez. 2020. "Synthesis of Hydroxyapatite-Ag Composite as Antimicrobial Agent". *Dose-Response*. Vol 18(3):1-14.

12. Kadouche, S., H. Lounici., K. Benaoumeur., N. Drouiche., M. Hadioui and P. Sharrock. 2012. "Enhancement of Sedimentation Velocity of Heavy Metals Loaded Hydroxyapatite Using Chitosan Extracted from Shrimp Waste". *Journal of Polymers and Environment*. Vol 20:848-857.

13. Kusnieruk, S., J. Wojnarowicz., A. Chodadra., T. Chudoba., S. Gierlotka and W. Lojkowski. 2016. "Influence of Hydrothermal Synthesis Parameters on The Properties of Hydroxyapatite Nanoparticles". *Beilstein Journal of Nanotechnology*. Vol 7:1586-1601.

14. LeGeros, R.Z. 1991. *Calcium Phosphates in Oral Biology*. Karger. Basel.

15. Lehninger, A.J. 1982. *Dasar-Dasar Biokimia Jilid I, Ed I*. Erlangga. Jakarta

16. Mirzaee, M., M. Vaezi and Y. Palizdae. 2016. "Synthesis and characterization of silver doped hydroxyapatite nanocomposite coatings and evaluation of their antibacterial and corrosion resistance properties in simulated body fluid". *Materials Science and Engineering C*. Vol 69:675-684.

17. Ngatijo., R. Bemis., Heriyanti., Rahmi., N. Ulwan and R. Basuki. 2021. "Synthesis and Characterization of Nano-sized Carbonated Calcium Hydroxyapatite (CHAp) from Rebon shrimp (*Acetes erythraeus*) as a Candidate for Dental Restoring Application". *Jurnal Kimia Valensi*. Vol 7(2):108-117.

18. Ni, Z., X. Gu., Y. He., Z. Wang., X. Zou., Y. Zhao and L. Sun. "Synthesis of silver nanoparticle-decorated hydroxyapatite (HA@Ag) poriferous nanocomposites and the study of their antibacterial activities". *RSC Advances*. Vol 8:41722-41730.

19. Pham, X.N., H.T. Nguyen and N.T. Pham. 2020. "Green Synthesis and Antibacterial Activity of Hap-Ag Nanocomposite Using *Centella asiatica* (L.) Urban Extraxt and Eggshell". *International Journal pf Biomaterials*. 1-12.

20. Prasetiowati, A.L., A.T. Prasetya and S. Wardani. 2018. "Sintesis Nanopartikel Perak dengan Bioreduktor Ekstrak Daun Belimbing Wuluh (*Averrhoa bilimbi L.*) sebagai Antibakteri". *Indonesian Journal of Chemical Science*. Vol 7(2):160-166.

21. Pribady, H.K., M. Ardana and R. Rusli. 2019. "Potensi Ekstrak Kulit Buah Pinang sebagai Antibateri *Propionibacterium acne* Penyebab Jerawat". *Proceeding of Mulawarman Pharmaceuticals Conferences*. Vol 10:100-103.

22. Said, M.M., M. Rehan., S.M El-Sheikh., M.K. Zahran., M.S.A. Aziz., M. Bechelany and A. Barhoum. 2021. "Multifunctional Hydroxyapatite/Silver Nanoparticles/Cotton Gauze for Antimicrobial and Biomedical Applications. *Nanomaterials*. Vol 11(2): 429.

23. Zakir, M., M.E.Y. Lembang and M.S Lembang. 2014. "Synthesis of Silver and Gold Nanoparticles through Reduction Method using Bioreductor of Leaf Extract of Ketapang (*Terminalia cattapa*)". *Presents in the International Conference on Advanced Material and Partical Nanotechnology*.